



Selective lysine-specific demethylase 1 inhibitor, NCL1, could cause testicular toxicity via the regulation of apoptosis

Satoshi Nozaki¹ | Taku Naiki¹  | Aya Naiki-Ito²  | Shoichiro Iwatsuki¹ | Tomoki Takeda¹ | Toshiki Etani¹ | Takashi Nagai¹ | Keitaro Iida¹ | Hiroyuki Kato² | Takayoshi Suzuki³ | Satoru Takahashi² | Yukihiro Umemoto^{1,4} | Takahiro Yasui¹

¹Department of Nephro-urology, Graduate School of Medical Sciences, Nagoya City University, Nagoya, Japan

²Department of Experimental Pathology and Tumor Biology, Graduate School of Medical Sciences, Nagoya City University, Nagoya, Japan

³Department of Complex Molecular Chemistry, The Institute of Scientific and Industrial Research, Osaka University, Suita, Japan

⁴Department of Education and Research Center for Advanced Medicine, Graduate School of Medical Sciences, Nagoya City University, Nagoya, Japan

Correspondence

Taku Naiki, Department of Nephro-urology, Graduate School of Medical Sciences, Nagoya City University, Kawasumi 1, Mizuho-cho, Mizuho-ku, Nagoya, Aichi 467-8601, Japan.
Email: naiki@med.nagoya-cu.ac.jp

Funding information

the Ministry of Education, Culture, Sports Science and Technology of Japan, Grant/Award Number: 18K16706

Abstract

Background: Recent studies have shown that epigenetic alterations, such as those involving lysine-specific demethylase 1 (LSD1), lead to oncogenic activation and highlight such alterations as therapeutic targets. However, studies evaluating the effect of LSD1 inhibitors on male fertility are lacking.

Objectives: We analyzed the potential toxicity of a new selective LSD1 inhibitor, N-[(1S)-3-[3-(trans-2-aminocyclopropyl)phenoxy]-1-(benzylcarbamoyl)propyl] benzamide (NCL1), in testes.

Materials and methods: Human testicular samples were immunohistochemically analyzed. Six-week-old male C57BL/6J mice were injected intraperitoneally with dimethyl sulfoxide vehicle (n = 15), or 1.0 (n = 15) or 3.0 (n = 15) mg/kg NCL1 biweekly. After five weeks, toxicity and gene expression were analyzed in testicular samples by ingenuity pathway analysis (IPA) using RNA sequence data and quantitative reverse transcriptase (qRT)-PCR; hormonal damage was analyzed in blood samples. NCL1 treated GC-1, TM3, and TM4 cell lines were analyzed by cell viability, chromatin immunoprecipitation, flow cytometry, and Western blot assays.

Results: LSD1 was mainly expressed in human Sertoli and germ cells, with LSD1 levels significantly decreased in a progressive meiosis-dependent manner; germ cells showed similar expression patterns in normal spermatogenesis and early/late maturation arrest. Histological examination revealed significantly increased levels of abnormal seminiferous tubules in 3.0 mg/kg NCL1-treated mice compared to control, with increased cellular detachment, sloughing, vacuolization, eosinophilic changes, and TUNEL-positive cells. IPA and qRT-PCR revealed NCL1 treatment down-regulated LSD1 activity. NCL1 also reduced total serum testosterone levels. Western blots of mouse testicular samples revealed NCL1 induced a marked elevation in cleaved caspases 3, 7, and 8, and connexin 43 proteins. NCL1 treatment significantly reduced GC-1, but not TM3 and TM4, cell viability in a dose-dependent manner. In flow cytometry analysis, NCL1 induced apoptosis in GC-1 cells.

This is an open access article under the terms of the Creative Commons Attribution-NonCommercial License, which permits use, distribution and reproduction in any medium, provided the original work is properly cited and is not used for commercial purposes.

© 2020 The Authors. *Andrology* published by Wiley Periodicals LLC on behalf of American Society of Andrology and European Academy of Andrology

Conclusions: High-dose NCL1 treatment targeting LSD1 caused dysfunctional spermatogenesis and induced caspase-dependent apoptosis. This suggests the LSD1 inhibitor may cause testicular toxicity via the regulation of apoptosis.

KEYWORDS

lysine-specific demethylase 1, NCL1, spermatogenesis, toxicity in testis

1 | INTRODUCTION

The incidence of malignant neoplasms in developed countries is growing, with nearly 70,000 people in the United States between the ages from 15 to 39 diagnosed with cancer each year.¹ Recently, patients in this age group, including a challenging population such as adolescents and young adults (AYA), have begun to be categorized in order to improve the distinct care provided by healthcare professionals.^{2,3} In addition, the National Comprehensive Cancer Network (NCCN) and American Society of Clinical Oncology (ASCO), among other important clinical cancer organizations, have introduced guidelines for the care of cancer survivors as well as have a role in educating clinicians and survivors, focusing their efforts on late effects and survivorship care.^{4,5} Nowadays, collaboration among oncology professionals is regarded as essential, with the existence of AYA oncology requiring further research in a diversity of fields, including infertility, through a coordinated approach.

Patients at an inoperative stage or with a hematological neoplasm tend to undergo systemic chemotherapy as standard treatment, mainly to extend overall survival; however, such cancer treatments have become diversified in recent years. Nowadays, new drugs targeting epigenetic alterations, which cause tumor suppression by attenuations of gene expression without being dependent on a DNA nucleotide sequence, have increasingly been used in a clinical setting.⁶ Most notably, lysine-specific demethylase 1 (LSD1), as a flavin-dependent enzyme, oxidatively demethylates monomethylated or demethylated bodies of residual lysines 4 or 9 on histone H3 protein (H3K4 and H3K9, respectively).⁷ H3K4 and H3K9 mediate many cellular signaling pathways⁸ and are involved in the initiation and development, in particular, of intractable cancers in the AYA generation. To date, many LSD1 inhibitors have been described and are undergoing clinical assessment.^{9,10} However, studies evaluating the impact of such LSD1 inhibitors on male fertility are lacking.

We have developed a novel selective LSD1 inhibitor N-[(1S)-3-[3-(trans-2-aminocyclopropyl)phenoxy]-1-(benzylcarbonyl)propyl]benzamide (NCL1), using both in vitro screening and protein structure similarity clustering,¹¹ and reported on the therapeutic efficacy of NCL1 using in vitro and in vivo models, and human samples of prostate cancer.^{12,13} In these analyses, we showed that LSD1 is highly expressed in normal mouse testes, however, there is a paucity of data concerning the expression and function of LSD1 in the testes, especially in humans. Therefore, in this study, we investigated the expression of LSD1 in human testicular specimens, including in

relation to normal spermatogenesis and spermatogenic dysfunction. In addition, we evaluated toxicity and the regulatory mechanisms of NCL1, especially from the viewpoint of treatment-related infertility both in vitro and in vivo, using RNA sequencing, flow cytometry, and western blot analyses.

2 | MATERIALS AND METHODS

2.1 | Human testicular samples

We obtained normal spermatogenesis specimens from five patients with obstructive azoospermia by testicular biopsy and spermatogenic dysfunctional specimens from a total of 20 patients who had non-obstructive azoospermia as revealed by microdissection testicular sperm extraction between 2013 and 2018. This study was approved by the Institutional Review Board at Nagoya City University Hospital (approval number 60-18-0153). All enrolled patients provided written informed consent and were assessed by a panel of experienced pathologists.

2.2 | Chemicals

NCL1 was synthesized as described in a previous paper.¹¹

2.3 | Animal procedures

Six-week-old male C57BL/6J mice were obtained from Nippon SLC and kept in plastic cages covered in hardwood chips in an air-conditioned, pathogen-free animal room at $22 \pm 2^\circ\text{C}$ and 50% humidity with a 12:12 h light/dark cycle. Then, intraperitoneal injections of vehicle control containing dimethyl sulfoxide (DMSO; equal to the concentration of DMSO for 3.0 mg/kg NCL1; $n = 15$), and 1.0 ($n = 15$) or 3.0 ($n = 15$) mg/kg NCL1 were performed twice weekly; the injection of 20 mg/kg busulfan ($n = 15$) as a positive control was performed once only. The measurement of body weights was performed twice weekly, and mice were euthanized 5 weeks after the start of injections. Blood samples were collected. Frozen samples of testes were obtained for the evaluation of testicular toxicity, and the analysis of protein expression at the termination of experiments. All experimental procedures were conducted according to protocols approved by the Institutional Animal Care and Use Committee

of Nagoya City University Graduate School of Medical Sciences (#H29M-63).

2.4 | Histological analysis

Immunohistochemical, and hematoxylin and eosin (HE) stains of 5- μ m thick paraffin-embedded testicular sections fixed in Bouin's fluid were carried out. Immunohistochemical staining was done automatically using BOND-MAX (Leica Microsystems). In human testicular specimens, at least 20 seminiferous tubules ($n = 5$ in each group) were evaluated. In vivo, at least from 30 to 50 round seminiferous tubules were randomly selected ($n = 15$ in each group), stages and types of abnormalities counted, and seminiferous tubule diameter measured. The relative intensities of LSD1 and connexin 43 (Cx43) were evaluated using a BZ-9000 microscope and its associated analytical software (Keyence Japan).

2.5 | Cell culture and reagents

GC-1, a mouse spermatogonia cell line, TM3, a mouse Leydig cell line, and TM4, a mouse Sertoli cell line were acquired from the American Type Culture Collection. GC-1 was maintained in Dulbecco's Modified Eagle's Medium (DMEM), with 10% fetal bovine serum (FBS), and 1% penicillin/streptomycin (P/S). TM3 and TM4 were maintained in DMEM: Nutrient Mixture F-12 (DMEM/F12), with 5% horse serum, 2.5% FBS, and 1% P/S (Thermo Fisher Scientific). All cells were maintained at 37°C in 5% CO₂ with humidity.

2.6 | Cell viability assay

Cell viability rates were measured using a Cell Counting Kit-8 (Dojindo Laboratories). GC-1, TM3, and TM4 cells were seeded into 96-well plates (5×10^3 cells/well) in their respective medium. After incubating overnight, the medium was changed and various concentrations of NCL1 added for 48 hours. Cell viability was evaluated by the absorption of WST-1, a tetrazolium dye.

2.7 | RNA extraction and quantitative reverse transcription-PCR (qRT-PCR)

Total RNA was isolated from each testis by phenol-chloroform extraction (Isogen; Nippon Gene Co. Ltd.). One microgram of RNA was converted to cDNA using avian myoblastosis virus reverse transcriptase (Takara) in 20 μ L reaction mixture. Aliquots of 2 μ L of cDNA samples were subjected to quantitative PCR (qPCR) in a total volume of 25 μ L using SYBR Premix ExTaq II (Takara) in a light cycler apparatus (Roche Diagnostic). The primers used were GAPDH F-TGAATACGGCTACAGCAACAGG,

R-GTGAGGGAGATGCTCAGTGTTG, Col1a2F-AACTCAGCTCGCTTCATGC, R-TTGTTCAAGCTGCCCGTCTC, Cdh1 F-CCGTCCTGCCAATCCTGATG, R-CTTCAGAACCCTGCCCCTCG, Hoxb7 F-AAGCATGAAACTCAAATAAAGGGGC, R-ACAAAAACAGACAACACAC TTTCCC, Scd1 F-CGAAGTCCACGCTCGATCTC, R-CGTTCAATTCCGGAGGGAGG, Lhcgr F-GATGCACAGTGGCACCTTC, R-TCAGCGTGGCAACCAGTAG, Hsd3b2 F-TCGGGACACTAGTGGAGCAG, R-AGCAGCACCTGTCTTGTGTG, and Clcn3 F-CTCATGTTGCTCTGCACCTCAC, R-AGGGACTGTAATGCGTCTCTGTG. GAPDH mRNA levels were used as internal controls.

2.8 | RNA purification and RNA-seq library preparation

RNA quality was evaluated with a Bioanalyzer RNA pico kit (Agilent Technologies). Based on the results of the quality check, RNA libraries were generated using Illumina's TruSeq Stranded Total RNA Sample Prep Kit using at least 100 ng of RNA. RNA libraries were multiplexed and sequenced with 150 bp-paired single-end reads (SR150) on an Illumina NovaSeq 6000.

2.9 | RNA sequencing data processing and analysis

First, the quality of the RNA sequencing (RNA-seq) data was assessed using FastQC ver.0.11.7 (<http://www.bioinformatics.babraham.ac.uk/projects/fastqc>). The reads were mapped to the reference genome using HiSat2 ver. 2.1.0. FeatureCounts ver. 1.6.3 was used to count the number of reads overlapping with each gene as specified in the genome annotation. Bioconductor package DESeq2 ver. 1.24.0 was used to test for differential gene expression between the experimental groups.

2.10 | Upstream regulator analyses

The Ingenuity Pathway Analysis tool (IPA; Ingenuity1 Systems) was used to assess upstream regulators. Only upstream regulators related to the epigenome were analyzed in the present study. Upstream regulators were predicted to be activated and inhibited for Z-scores.

2.11 | Flow cytometry analysis for the detection of apoptosis

TM3, TM4, and GC-1 cells were treated with NCL1 for 48 hours. A Guava® easyCyte system (Luminex Corporation) was used as an apoptosis assay. A phycoerythrin Annexin V Apoptosis Detection Kit with 7-aminoactinomycin D (BioLegend) was used as an apoptosis assay in accordance with the manufacturer's instructions.

2.12 | Western blot analysis

Whole-cell protein extracts from mouse testicular samples after the removal of the tunica albuginea *in vivo*, and GC-1, TM3, and TM4 cells *in vitro* were used. The 30 μ g of protein in each sample was resolved in a 12.5% polyacrylamide gel and transferred onto polyvinylidene fluoride microporous membranes. Signals were detected using an Amersham chemiluminescence Western Blotting Detection Reagent (GE Healthcare Life Sciences). Chemiluminescent signals were scanned using a LAS 4000 mini analyzer (GE Healthcare). Antibodies against LSD1 (1:500; Cell Signaling Technology), androgen receptor (1:500; AR; Abcam), Cx43 (1:500; Cell Signaling Technology), H3K4me1 (1:500; Active Motif), di-methylated H3K4 (H3K4me2; 1:500; Cell Signaling Technology), cleaved caspases 3, 7, 8, 9 (1:500; Cell Signaling Technology), and Oct4 (1:250; Abcam) were used to detect protein levels. Anti-beta-actin antibody (Mab; Sigma-Aldrich) was used to detect beta-actin protein used as a protein loading control.

2.13 | TUNEL assay

A terminal deoxy nucleotidyl transferase-mediated dUTP nick end labeling (TUNEL) assay was performed with an In Situ Apoptosis Detection Kit to detect apoptotic cells in deparaffinized tissues according to the manufacturer's instructions. The relative ratio of TUNEL-positive cells was determined from five random microscopic fields in tissues from each group.

2.14 | Chromatin immunoprecipitation assay followed by real-time PCR

GC-1 cells were cultivated for 16 hours in the presence or absence of 30 μ M NCL1 as indicated. Then, cells were cross-linked using 1% formaldehyde, and the chromatin was subjected to chromatin immunoprecipitation assay (ChIP) using an H3K4-me2 antibody (1:50; Cell Signaling). Isotype-specific IgG was used as a control. Extracted DNA was dissolved in TE buffer and subjected to real-time PCR using Oct4 specific primers: primer A F-TGGTTGCAAAGCCAGTCACTA, R-TGACTACTGGCCAGGACAA; and primer B F-CCCTTGAA CCTGAAGTCAGATATTT, R- GCCTAGTTCCTGGGTGGAGAA.

2.15 | Statistical analysis

Student's *t* test was used to assess the associations between different variables and a one-way analysis of variance ANOVA followed by Dunnett's post hoc test was used, when appropriate, using EZR software version 1.40 (Jichi Medical University Saitama Medical Center).¹⁴ $P < .05$ was regarded as statistically significant.

3 | RESULTS

3.1 | LSD1 expression in human testicular samples

For the analysis of LSD1 expression in human testicular samples, we obtained normal spermatogenesis (NS) specimens ($n = 5$) as well as specimens in various degrees of spermatogenetic dysfunction ($n = 25$). According to a panel of experienced pathologists, the abnormal specimens were categorized as late maturation arrest (late MA), in which spermatids were detected without spermatozoa, early maturation arrest (early MA), in which cells are not present except for spermatogonia or spermatocytes, and Sertoli cell-only (SCO), in which only Sertoli cells were found. LSD1 protein localization and expression levels in testicular cells were quantified using BZ-9000 multifunctional microscopy. LSD1 was found to be mainly expressed in Sertoli cells, spermatogonia, spermatocytes, round and elongated spermatids, and spermatozoa (Figure 1A-H). In an analysis according to the various degrees of tubular degeneration, the intensity of LSD1 in Sertoli cells was highly maintained. In addition, among germ cells, intensity levels were significantly decreased in a progressive meiosis-dependent manner. Furthermore, expression patterns among germ cells were similar in NS, late MA, and early MA (Figure 1I).

3.2 | Analysis of testicular toxicity induced by NCL1 treatment in an *in vivo* model

For the evaluation of testicular toxicity of NCL1 *in vivo*, we used busulfan, a compound widely known to induce testicular toxicity, as a positive control. The dose of busulfan was determined based on a previous study.¹⁵ As shown in the Table 1, significant changes in body weight were not found between the four treatment groups. The average relative testicular weight of animals in the busulfan group was significantly smaller than that of the control group. However, a difference between control and NCL1 3.0 mg/kg treatment groups was not found. Total serum testosterone levels were significantly decreased in NCL1 treatment groups compared with the vehicle control group (Table 1). Histological examination revealed that the proportion of abnormal seminiferous tubules in animals of the busulfan and NCL1 3.0 mg/kg groups was significantly greater than in animals of the vehicle control group (Figure 2A-E). For normal seminiferous tubules, the constitutive ratios for the various stages of spermatogenesis were not statistically different between the four groups (Figure 2F). Therefore, we further analyzed the categorization of abnormal seminiferous tubules in previous reports.¹⁶ For the busulfan group, the percentages of cells showing detachment, sloughing, or vacuolization were significantly higher compared with that found in the control group. For NCL1 treatment groups, as with the busulfan group, in addition to the higher levels of cells showing detachment, sloughing and vacuolization,

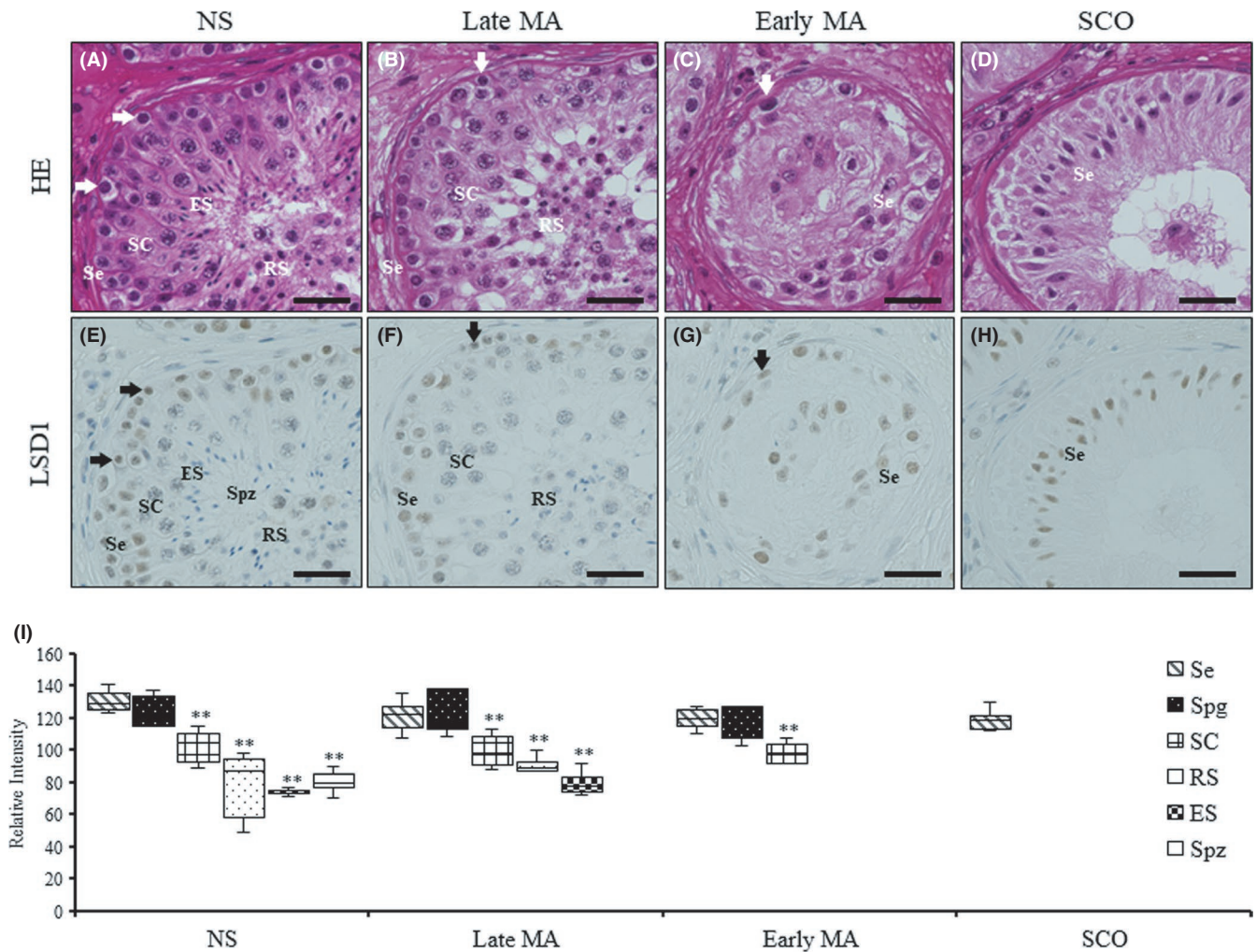


FIGURE 1 Histological analysis of human testis from normal spermatogenesis (NS), late maturation arrest (late MA), early maturation arrest (early MA), and Sertoli cell-only (SCO) groups. Arrows indicate spermatogonia. Se, Sertoli cells; Spg, spermatogonia; SC, spermatocytes; RS, round spermatids; ES, elongated spermatids; Spz, spermatozoa. (A-D), Hematoxylin and eosin (HE) staining; (E-H), immunohistochemistry staining for LSD1. Scale bar indicates 40 μ m. (I), Relative intensity of lysine-specific demethylase 1 (LSD1) in each cell type. Mean \pm standard deviation (SD). ** $P < .01$, statistically significant compared to spermatogonia group

TABLE 1 Body weights, testicular weights and blood testosterone levels in mice treated with busulfan or NCL1

	No. of mice	Body weight (g)	Average of relative testicular weight (%)	Total testosterone levels (ng/mL)
Control	15	25.7 \pm 0.22	4.53 \pm 0.29	15.0 \pm 16.6
Busulfan	15	25.3 \pm 0.45	3.20 \pm 0.56**	1.79 \pm 4.00**
NCL1 1.0 mg/kg	15	27.2 \pm 1.46	4.20 \pm 0.24	3.10 \pm 6.85 [†]
NCL1 3.0 mg/kg	15	25.1 \pm 1.31	4.55 \pm 0.32	3.93 \pm 8.01 [†]

Note: NCL1, N-[(1S)-3-[3-(trans-2-aminocyclopropyl)phenoxy]-1-(benzylcarbamoyl)propyl]benzamide; Mean \pm standard deviation (SD).

[†] $P < .05$;

** $P < .01$

eosinophilic changes were significantly higher compared with cells in the testes of vehicle control group animals Figure 2G. Seminiferous tubule diameters were significantly shorter in the busulfan compared to vehicle control group, however, NCL1 treatment groups did not show a difference compared with vehicle control Figure 2H.

3.3 | IPA analysis by RNA sequence data and the confirmation of degradation of LSD1 activity in an in vivo model

For the determination of LSD1 activity induced by NCL1 treatment, we further explored possible signaling pathways regulated by LSD1.

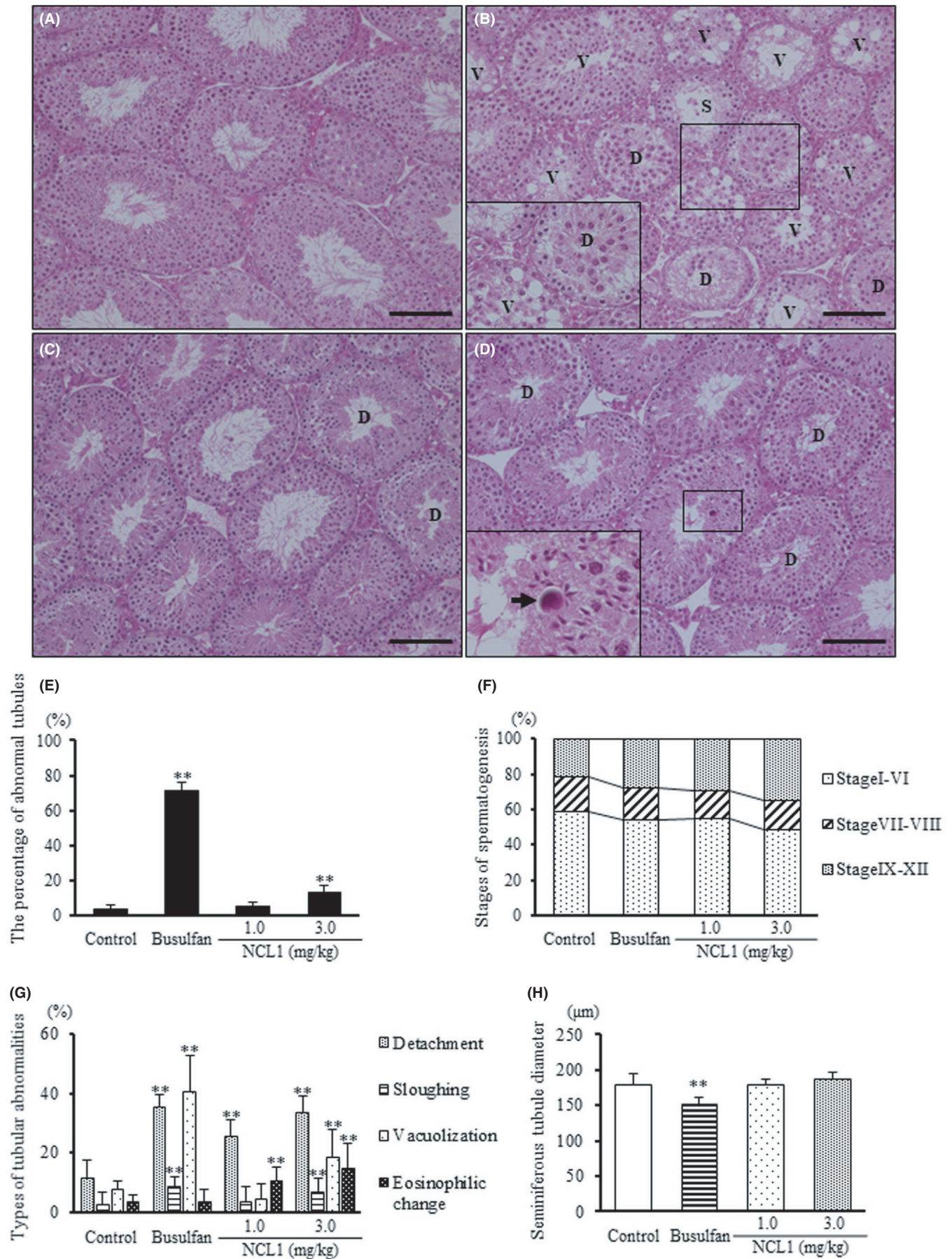


FIGURE 2 Hematoxylin and eosin (HE) staining of mice testis from vehicle control (A), busulfan (B), NCL1 1.0 mg/kg (C), and NCL1 3.0 mg/kg (D) groups. The arrows indicate eosinophilic change. D, detachment; S, sloughing; V, vacuolization. Scale bars indicate 100 μ m. (E), The percentage of abnormal tubules. Abnormal tubules were defined as showing a depletion of spermatids. (F), Constitutive ratios for stages of spermatogenesis. Tubules were classified into three stages: stage I-VI, VII-VIII, and IX-XII. (G), The percentage of abnormal tubules with detachment, sloughing, vacuolization, and eosinophilic change in control and treated groups. (H), Seminiferous tubule diameter in control and treated groups. Mean \pm standard deviation (SD); $^{*}P < .01$, statistically significant compared to control group. NCL1 (N-[(1S)-3-[3-(trans-2-aminocyclopropyl)phenoxy]-1-(benzylcarbamoyl)propyl] benzamide

The gene expression changes between testes in in vivo testicular samples after NCL1 treatment and controls were analyzed by RNA sequencing and IPA software. IPA analysis revealed signaling pathways associated with LSD1 were significantly down-regulated Figure 3A. qRT-PCR revealed that mRNA expression of *Colla2*, *Cdh1*, *Hoxb7*, and *Scd1* was significantly changed, similar to RNA sequence data Figure 3B-E. These results indicate that LSD1 activity and pathways were down-regulated by NCL1 treatment. In addition, of mRNAs down-regulated by NCL1 treatment, the regulatory pathway relating to the synthesis of testosterone was attenuated

Figure 3A. qRT-PCR revealed that *Lhcgr*, *Hsd3b2*, and *Cln3* were also significantly changed, similar to RNA sequence data, by NCL1 treatment as compared to control Figure 3F-H).

3.4 | In vivo regulation of testicular degeneration by NCL1

We then examined LSD1 protein expression and the regulatory mechanisms of NCL1 in the testis after treatments in an in vivo model. We

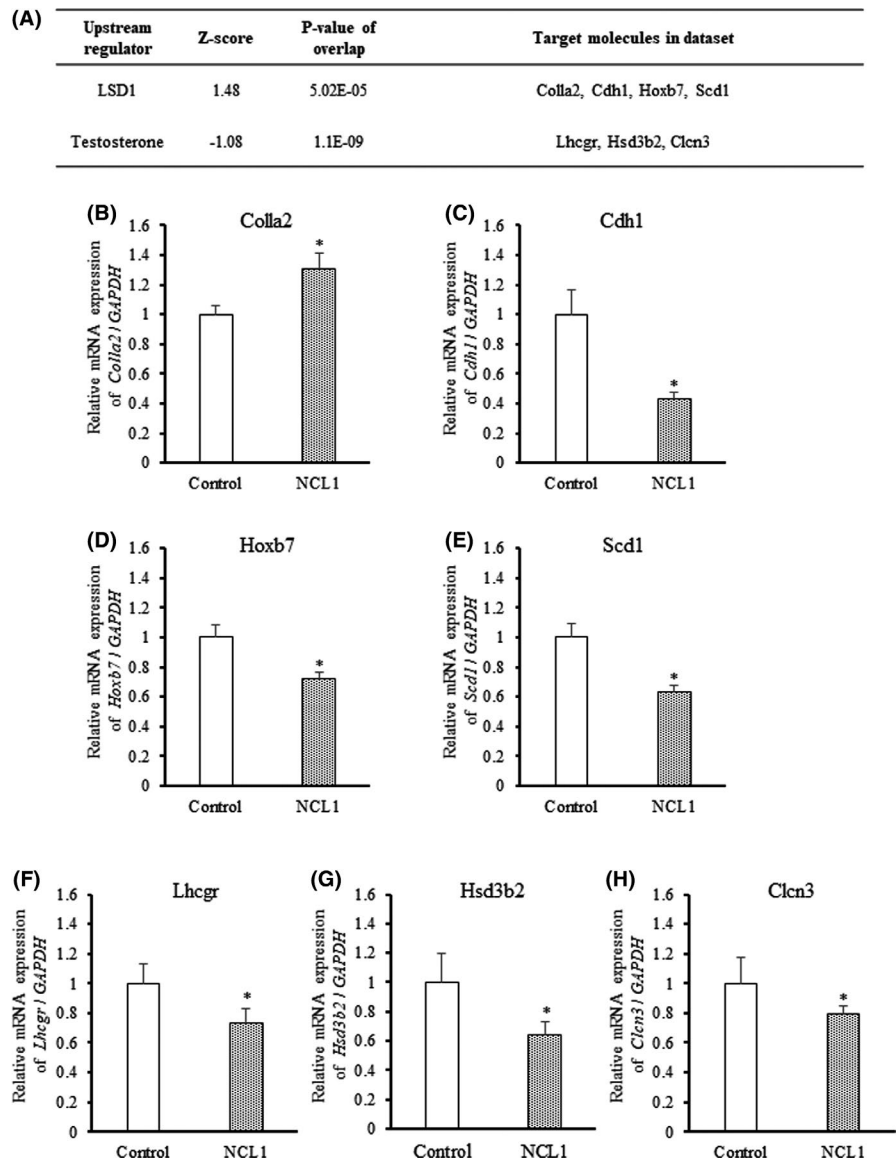


FIGURE 3 (A), Ingenuity pathway analysis using RNA sequence data. The Z-score was an indicator of the certainty of activation or inhibition; a high Z-score indicates a high certainty of activation. Quantitative reverse transcriptase PCR of *Colla2* (B), *Cdh1* (C), *Hoxb7* (D), *Scd1* (E), *Lhcgr* (F), *Hsd3b2* (G), and *Cln3* (H) mRNAs in NCL1 treated and vehicle control groups is shown (n = 8 in each group). Mean \pm standard error of mean (SE); $^{*}P < .05$, statistically significant. LSD1, lysine-specific demethylase 1; NCL1 (N-[(1S)-3-[3-(trans-2-aminocyclopropyl)phenoxy]-1-(benzylcarbamoyl)propyl] benzamide

FIGURE 4 (A-C), Immunohistochemistry staining for lysine-specific demethylase 1 (LSD1) in mice testes from vehicle control (A), busulfan (B), and NCL1 3.0 mg/kg (C) groups. (D-H), Terminal deoxynucleotidyl transferase-mediated dUTP nick end labeling (TUNEL) staining for apoptosis in mice testes from vehicle control (D), busulfan (E), NCL1 1.0 mg/kg (F), and NCL1 3.0 mg/kg (G) groups. Arrowheads indicate TUNEL-positive cells. Scale bars indicate 100 μ m. (H), Percentage of seminiferous tubules presenting with TUNEL-positive cells. Mean \pm standard deviation (SD); ** $P < .01$ compared to control group. (I), Western blot analyses following vehicle control, busulfan, or NCL1 3.0 mg/kg treatment using anti-LSD1, anti-androgen receptor (AR), anti-connexin 43 (Cx43), anti-histone H3 lysine 4 mono/dimethyl (H3K4me1/me2), and anti-cleaved caspase (CCas) 3/7/8/9 antibodies. ($n = 3$ in each group). (J-M), Immunohistochemistry staining for Cx43 in mice testes from vehicle control (J) and NCL1 3.0 mg/kg (K) groups. Arrowheads indicate Leydig cell nodules. Scale bars indicate 40 μ m. (L), Area of Leydig cell nodules. (M), Relative intensity of Cx43. Mean \pm standard deviation (SD); ** $P < .01$, statistically significant. NCL1 (N-[[1S]-3-[3-(trans-2-aminocyclopropyl)phenoxy]-1-(benzylcarbamoyl)propyl] benzamide

found that the localization and high level of LSD1 expression did not differ between groups Figure 4A-C. In addition, in the assessment of the regulatory mechanism of NCL1, TUNEL assays revealed that the administration of 3.0 mg/kg NCL1 significantly increased the percentage of seminiferous tubules that presented with TUNEL-positive cells compared with vehicle control, busulfan and NCL1 1.0 mg/kg remained unchanged compared to vehicle control Figure 4D-H). In western blot analysis, the expression of H3K4me2, reflecting methylation status, was increased after treatment with NCL1 compared with vehicle control and treatment with busulfan, the expression of H3K4me1 was decreased with NCL1 treatment Figure 4I. Western blot analysis also showed that NCL1 treatment induced a marked elevation in cleaved caspases 3, 7, and 8 compared with busulfan or vehicle control groups Figure 4I. Furthermore, NCL1 and busulfan treatment caused a marked elevation in Cx43 expression, a testicular gap junction protein Figure 4I. In addition, after performing immunohistochemistry for Cx43, we found Cx43 staining mainly in Leydig cells Figure 4J,K). The area of Leydig cells clustered in the interstitial space was significantly enlarged in the NCL1 treated compared to control group Figure 4L. The intensity of Cx43 staining remained unchanged between control and NCL1 treatment groups Figure 4M.

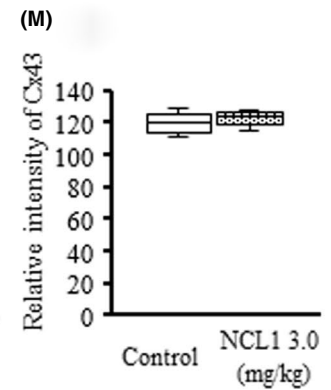
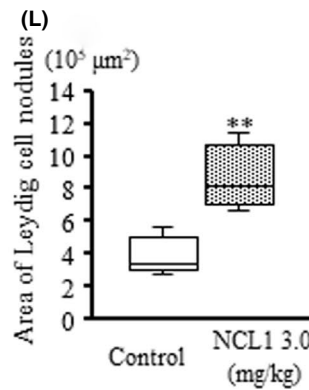
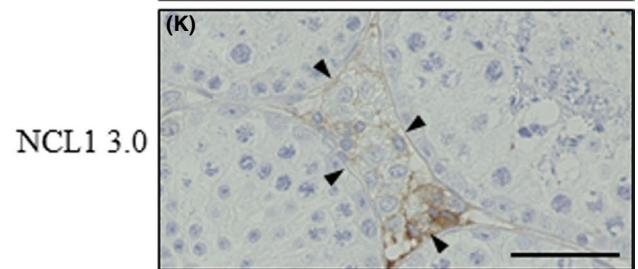
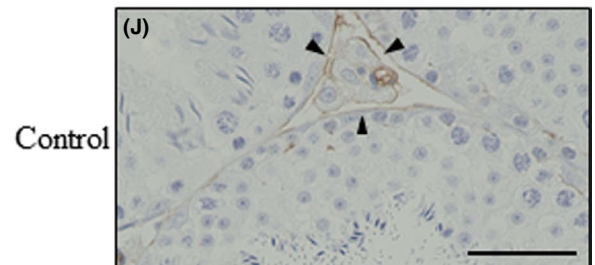
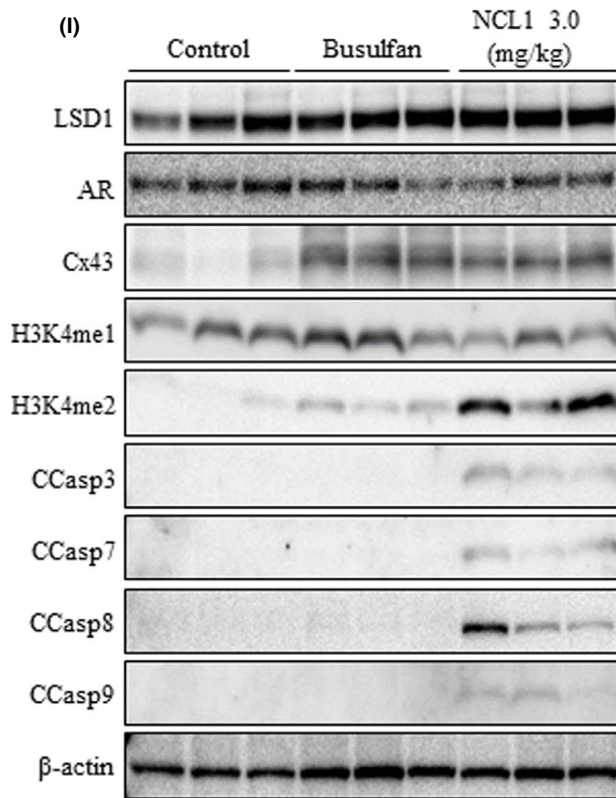
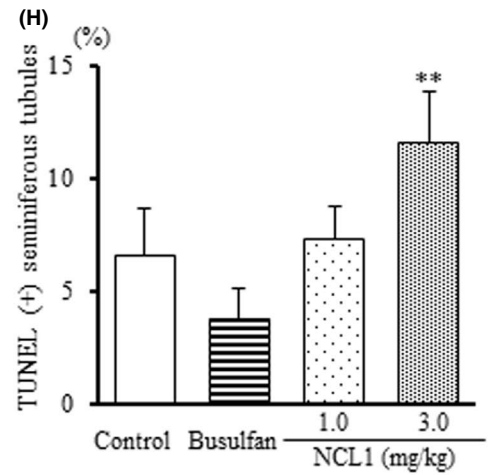
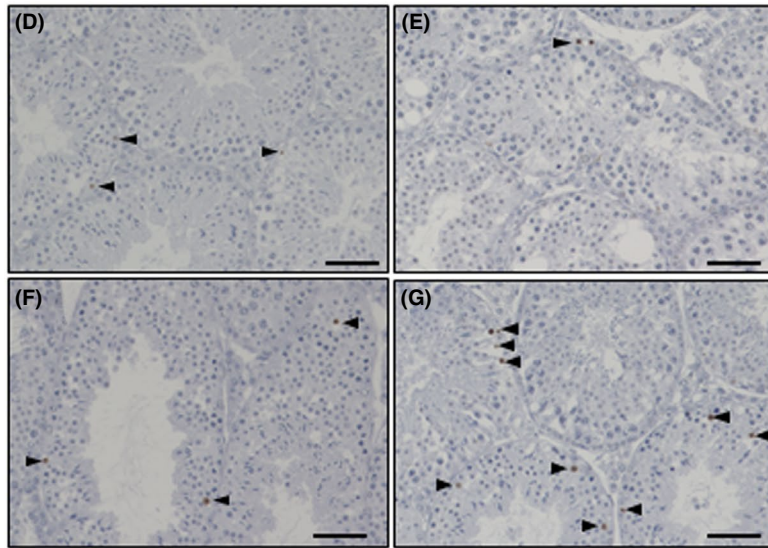
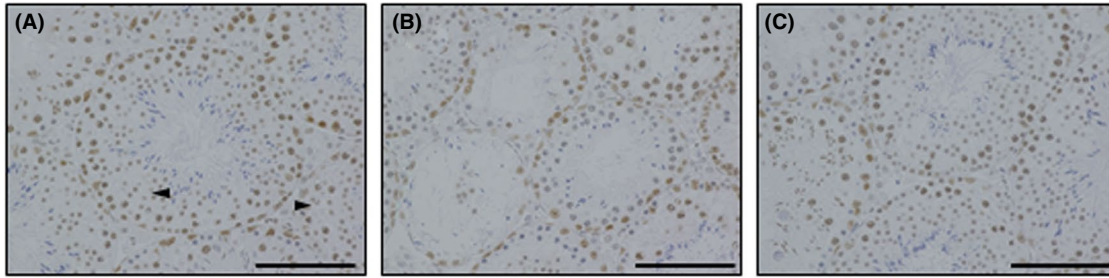
3.5 | NCL1 treatment induced apoptosis in testicular cell lines

LSD1 was examined in testicular cells in vitro. Western blot analysis revealed that LSD1 protein was highly expressed in GC-1, TM3, and TM4 cell lines Figure 5A. In addition, the localization of LSD1 protein occurred only in the nucleus for all three cell lines Figure 5B. To determine whether LSD1 inhibition influenced gene-specific methylation status, GC-1 cells treated with NCL1 were subjected to ChIP assay. Evidence exists that histone H3 methylation underlies the control of expression of *Oct4*, one of the key genes in spermatogenesis in GC-1 cells.¹⁷ The mouse *Oct4* promoter has been well characterized and comprises defined regulatory regions that are critical for activation.¹⁸ To identify epigenetic changes in the *Oct4* promoter, primers A (-2281 to -2212 relative to TSS) and B (-854 to -781 relative to TSS) were used in qRT-PCR analyses.¹⁷ It was found that NCL1 specifically impaired the demethylation of H3K4me2 in the containing promoter lesion of the *Oct4* gene Figure 5C, reflecting the increased level of fold enrichment compared with IgG control in a ChIP assay, and decreased levels of *Oct4* protein expression in

western blot analysis compared to control. To evaluate the role of LSD1 in testicular cells in vitro, a cell viability assay and Guava apoptosis[®] analysis were performed. The cell viability of the GC-1 cell line was found to be significantly reduced in a dose-dependent manner with NCL1 treatment Figure 5D; however, differences in TM3 and TM4 cell lines with NCL1 treatment were not observed Figure 5G,J). In a Guava[®] apoptosis analysis, NCL1 induced apoptosis in the GC-1 cell line compared to vehicle control Figure 5E,F but TM3 and TM4 remained unaffected Figure 5H,I,K,L).

4 | DISCUSSION

The process of spermatogenesis requires complicated regulation of differentiation in multiple cells with changes in chromatin structure and gene transcription. Additionally, the epigenetic regulatory mechanisms in spermatogenesis have gradually been elucidated.^{19,20} Recently, it was shown that conditional deletion of LSD1 in the mouse testis prior to birth led to fewer spermatogonia as well as germ cell loss before three weeks of age.²¹ Moreover, using an LSD1 conditional knockout mouse model, it was shown that LSD1 has a critical role in maintenance during the first wave of spermatogenesis.²² However, reports on LSD1 expression in the human testis are lacking. In this study, immunohistochemical analyses revealed various degrees of tubular degeneration in testicular samples. In Sertoli cells, the intensity of LSD1 was highly maintained. In germ cells, intensity levels were significantly decreased in a meiosis-dependent, progressive manner. In addition, histological examination in our in vivo study revealed that abnormal seminiferous tubules in response to treatment with busulfan and 3.0 mg/kg NCL1 were significantly increased compared to the vehicle control group. Total testosterone levels in serum were significantly decreased in NCL1 treatment groups compared with the vehicle control group. Furthermore, in IPA by RNA sequencing, an upstream regulator gene in testosterone synthesis was attenuated by NCL1 treatment, and mRNA levels of *Lhcgr* and *Hsd3b2* were significantly decreased. These genes are important regulators of testosterone synthesis, particularly in Leydig cells. Therefore, a possible reason for testosterone reduction induced by NCL1 treatment could be as a direct effect on Leydig cells via the LSD1 pathway. These results suggest that, irrespective of the degree of tubular degeneration, an LSD1 inhibitor can cause severe toxicity in spermatogenesis. Therefore, when using new drugs targeting LSD1 in patients of the AYA generation, such



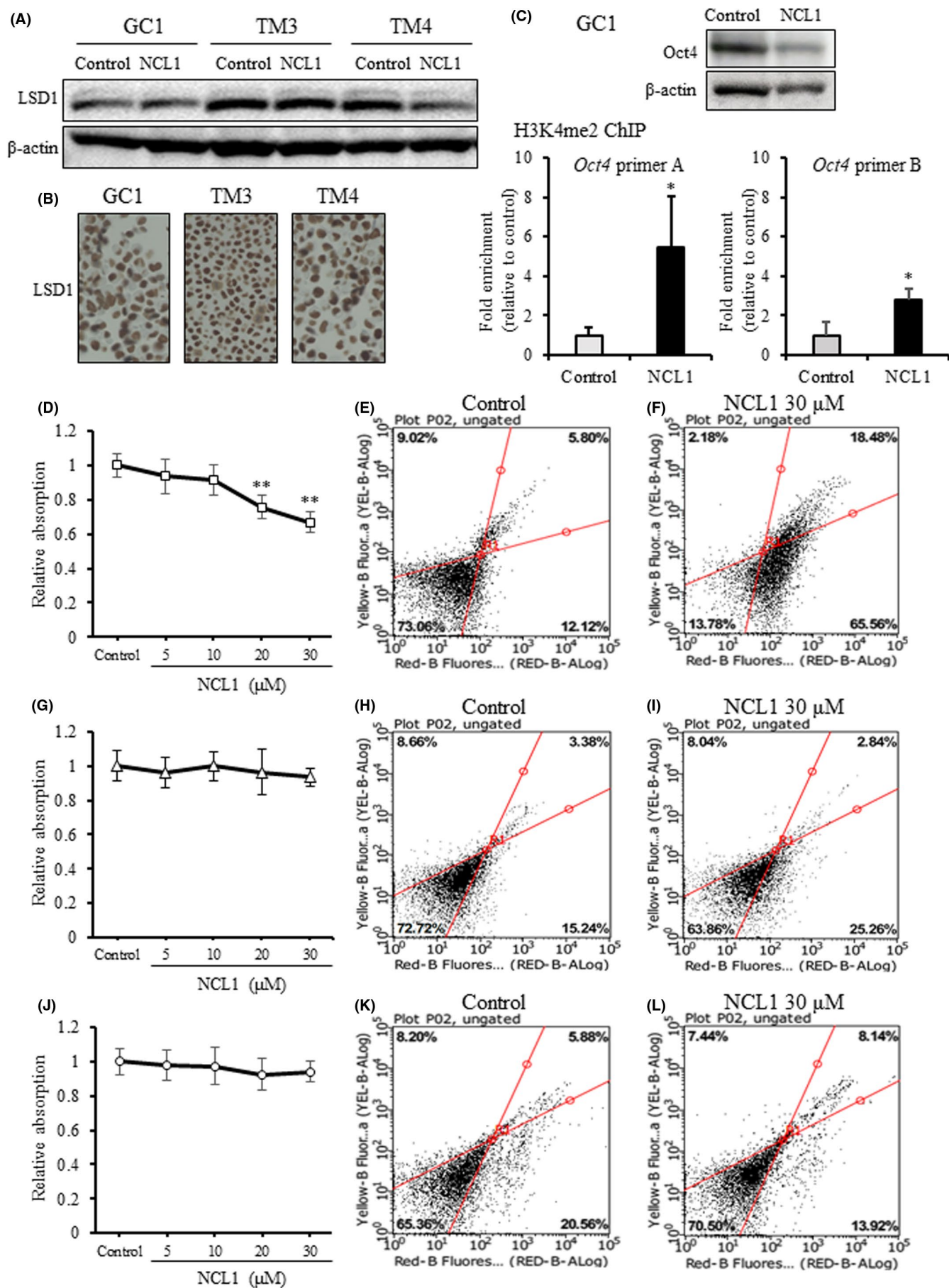


FIGURE 5 (A), Western blot analysis of lysine-specific demethylase 1 (LSD1) in GC-1, TM3, and TM4 cell lines after treatment with vehicle control or 30 μ M NCL1. (B), Immunohistochemical analysis of LSD1 in the three cell lines. (C), Chromatin immunoprecipitation (ChIP) analysis using an H3K9me2 antibody. Western blot analysis of Oct4 protein and the accumulation of H3K9me2 in the promoter region of the Oct4 gene in GC-1 cells after treatment with vehicle control or NCL1. Mean \pm standard error of mean (SE); * P < .05, statistically significant. Cell viability assays. GC-1 (D), TM3 (G), and TM4 (J) cells were seeded in 96-well plates, treated with vehicle control or NCL1, and subjected to a Cell Counting Kit-8 after 48 hours. Mean \pm standard deviation (SD); ** P < .01, statistically significant. Guava apoptosis[®] analysis of GC-1 (E, F), TM3 (H, I), and TM4 (K, L) cells. NCL1 (N-[(1S)-3-[3-(trans-2-aminocyclopropyl)phenoxy]-1-(benzylcarbamoyl)propyl] benzamide

information, including ASCO and NCCN guidelines with reference to infertility, should be noted.

Many chemotherapeutic agents can cause temporary or permanent toxicity leading to treatment-related infertility. Rates of permanent infertility and compromised treatment-related infertility vary as reported within the literature.^{23,24} Many factors, including the pharmacological effect of such agents and the administered dose, can affect male reproductive ability by, for example, affecting hormonal secretion via the central nervous system, having direct gonadotoxic effects, or by affecting spermatozoa or sexual function. In previous reports, agents were categorized into three risk classifications. For example, methotrexate, fluorouracil vincristine, bleomycin, and dactinomycin were associated with low gonadotoxicity.²⁵⁻²⁷

More recently, molecular-targeting therapies, including tyrosine kinase inhibitors and tumor-specific monoclonal antibodies, are increasingly being used. However, studies of the effect of such new drugs on male infertility are limited compared with those involving chemotherapeutic agents.^{24,28} Of these, studies of the effects of imatinib, an inhibitor targeting tyrosine kinases, on spermatogenesis in rodent models showed positive and negative conflicting results. A study using rats revealed that the administration of imatinib did not induce toxicity in the testis,²⁹ whereas another study using mice demonstrated an elevation in gonadotropins after treatment.³⁰ To date, speculation about treatment-related infertility caused by newly investigated drugs has been derived from data from in vivo experiments using animal models.

In our study, we used busulfan as a positive control. Busulfan is a common alkylating drug for chronic myeloid leukemia that is widely used before the transplantation of hematopoietic stem cells^{31,32} and has been categorized in a high-risk group in previous studies. We used two doses of NCL1: a high dose of 3.0 mg/kg, and a low dose of 1.0 mg/kg, the latter was previously reported by us as a therapeutic dose.¹² We found that high-dose NCL1 targeting LSD1 treatment caused a high incidence of abnormal seminiferous tubules and a decrease in serum total testosterone levels similar to busulfan treatment. It was striking that histological analyses by experienced pathologists revealed that the patterns of tubular abnormalities differed between NCL1 and busulfan treatments, however, the seminiferous tubule diameter remained unchanged in NCL1 treatment. In addition, one of the mechanisms of dysgenesis caused by NCL1 was revealed to be by caspase-dependent apoptosis. Further research in future investigating long-term treatment and/or long-term follow-up without treatment would clarify whether the effects caused by NCL1 are temporary or permanent.

As a major gap junction protein, connexin is expressed in testis in addition to connexins 26, 32, and 33. To date, the intricacies of intercellular communication, especially via Cx43 gap junctions in the testis, are well established. Cx43 has a pivotal role in developing germ cells throughout fetal development and spermatogenesis in the adult.^{33,34} In particular, the gap junction is a component of the blood-testis barrier in addition to tight junctions. Studies have shown that Cx43 gap junctions need to be established between cells in Sertoli cell differentiation regulated by thyroid hormones.³⁵ However, because Cx43 knockout mouse testes showed normal Leydig cells and can secrete androgen after luteinizing hormone stimulation, Cx43 may not be required for Leydig cell proliferation or differentiation.³³ In a previous report, when cell death was induced in hepatocytes, Cx43 was highly upregulated in the cell cytoplasm in a gap junction-independent manner.^{36,37} In our study, NCL1 and busulfan treatment caused a marked elevation in Cx43 expression. Immunohistochemical analyses in vivo found that Cx43 was mainly localized in Leydig cells. An enlargement of the area of Leydig cell clusters in the interstitial space was the main reason for the overexpression of Cx43 after NCL1 treatment. The role of Cx43 in cell death in Leydig cells is not fully understood. However, similar mechanisms, such as found in hepatocytes responding to cell death via the overexpression of Cx43, may occur at an intermediate level in testicular toxicity. More detailed studies are needed to investigate other mechanisms.

Considering the current circumstance in that the way to avoid treatment-related infertility is mainly by the preservation of spermatozoa in advance of treatments, a lot of validated information from in vivo experiments and human clinical data remains to be accumulated. In our study, high-dose NCL1 targeting LSD1 caused dysfunctional spermatogenesis and a decrease in serum total testosterone levels similar to that observed during busulfan treatment. We hope these findings contribute to the future development of novel potential therapeutic agents targeting LSD1 in patients of the AYA generation.

ACKNOWLEDGMENTS

This work was supported in part by a Grant-Aid from the Ministry of Education, Culture, Sports Science and Technology of Japan (grant number 18K16706).

CONFLICT OF INTEREST

The authors state that they have no potential conflicts of interest to declare.

ORCID

Taku Naiki  <https://orcid.org/0000-0002-7638-6048>

Aya Naiki-Ito  <https://orcid.org/0000-0003-0828-2033>

REFERENCES

- Kelvin JF. Fertility preservation in young adult patients with cancer. *Oncology*. 2017;31:530, 534-536, 538, 570.
- Bleyer A. Young adult oncology: the patients and their survival challenges. *CA Cancer J Clin*. 2007;57:242-255.
- Burkart M, Sanford S, Dinner S, Sharp L, Kinahan K. Future health of AYA survivors. *Pediatr Blood Cancer*. 2019;66:e27516.
- Oktay K, Harvey BE, Partridge AH, et al. Fertility preservation in patients with cancer: ASCO clinical practice guideline update. *J Clin Oncol*. 2018;36:1994-2001.
- Coccia PF, Pappo AS, Beaupin L, et al. Adolescent and Young Adult Oncology, Version 2.2018, NCCN Clinical Practice Guidelines in Oncology. *J Natl Compr Canc Netw*. 2018;16:66-97.
- Kelly AD, Issa J-PJ. The promise of epigenetic therapy: reprogramming the cancer epigenome. *Curr Opin Genet Dev*. 2017;42:68-77.
- Shi Y, Lan F, Matson C, et al. Histone demethylation mediated by the nuclear amine oxidase homolog LSD1. *Cell*. 2004;119:941-953.
- Hamamoto R, Saloura V, Nakamura Y. Critical roles of non-histone protein lysine methylation in human tumorigenesis. *Nat Rev Cancer*. 2015;15:110-124.
- Przespolewski A, Wang ES. Inhibitors of LSD1 as a potential therapy for acute myeloid leukemia. *Expert Opin Investig Drugs*. 2016;25:771-780.
- Fu X, Zhang P, Yu B. Advances toward LSD1 inhibitors for cancer therapy. *Future Med Chem*. 2017;9:1227-1242.
- Ueda R, Suzuki T, Mino K, et al. Identification of Cell-Active Lysine Specific Demethylase 1-Selective Inhibitors. *J Am Chem Soc*. 2009;131:17536-17537.
- Etani T, Suzuki T, Naiki T, et al. NCL1, a highly selective lysine-specific demethylase 1 inhibitor, suppresses prostate cancer without adverse effect. *Oncotarget*. 2015;6:2865-2878.
- Etani T, Naiki T, Naiki-Ito A, et al. NCL1, a highly selective lysine-specific demethylase 1 inhibitor, suppresses castration-resistant prostate cancer growth via regulation of apoptosis and autophagy. *J Clin Med*. 2019;8:442.
- Kanda Y. Investigation of the freely available easy-to-use software 'EZR' for medical statistics. *Bone Marrow Transplant*. 2013;48:452-458.
- Anjamrooz SH, Movahedin M, Mowla SJ, Bairanvand SP. Assessment of morphological and functional changes in the mouse testis and epididymal sperms following busulfan treatment. *Iran Biomed J*. 2007;11:15-22.
- Khorsandi L, Oroojan AA. Toxic effect of *Tropaeolum majus* L. leaves on spermatogenesis in mice. *JBRA Assist Reprod*. 2018;22:174-179.
- Godmann M, May E, Kimmins S. Epigenetic mechanisms regulate stem cell expressed genes Pou5f1 and Gfra1 in a male germ cell line. *PLoS One*. 2010;14:e12727.
- Yeom YI, Fuhrmann G, Ovitt CE, et al. Germline regulatory element of Oct-4 specific for the totipotent cycle of embryonal cells. *Development*. 1996;122:881-894.
- Godmann M, Auger V, Ferraroni-Aguiar V, et al. Dynamic Regulation of Histone H3 Methylation at Lysine 4 in Mammalian Spermatogenesis1. *Biol Reprod*. 2007;77:754-764.
- Zhang L, Wang J, Pan Y, et al. Expression of histone H3 lysine 4 methylation and its demethylases in the developing mouse testis. *Cell Tissue Res*. 2014;358:875-883.
- Myrick DA, Christopher MA, Scott AM, et al. KDM1A/LSD1 regulates the differentiation and maintenance of spermatogonia in mice. *PLoS One*. 2017;12:e0177473.
- Lambrot R, Lafleur C, Kimmins S. The histone demethylase KDM1A is essential for the maintenance and differentiation of spermatogonial stem cells and progenitors. *FASEB J*. 2015;29:4402-4416.
- Howell SJ, Shalet SM. Testicular function following chemotherapy. *Hum Reprod Update*. 2001;7:363-369.
- Samplaski MK, Nangia AK. Adverse effects of common medications on male fertility. *Nat Rev Urol*. 2015;12:401-413.
- Wallace WHB, Anderson RA, Irvine DS. Fertility preservation for young patients with cancer: who is at risk and what can be offered? *Lancet Oncol*. 2005;6:209-218.
- Lee SJ, Schover LR, Partridge AH, et al. American Society of Clinical Oncology recommendations on fertility preservation in cancer patients. *J Clin Oncol*. 2006;24:2917-2931.
- Brydøy M, Fosså SD, Dahl O, Bjørø T. Gonadal dysfunction and fertility problems in cancer survivors. *Acta Oncol (Madr)*. 2007;46:480-489.
- Loren AW, Mangu PB, Beck LN, et al. Fertility Preservation for Patients With Cancer: American Society of Clinical Oncology Clinical Practice Guideline Update. *J Clin Oncol*. 2013;31:2500-2510.
- Schultheis B, Nijmeijer BA, Yin H, Gosden RG, Melo JV. Imatinib mesylate at therapeutic doses has no impact on folliculogenesis or spermatogenesis in a leukaemic mouse model. *Leuk Res*. 2012;36:271-274.
- Nurmio M, Kallio J, Toppari J, Jahnukainen K. Adult reproductive functions after early postnatal inhibition by imatinib of the two receptor tyrosine kinases, c-kit and PDGFR, in the rat testis. *Reprod Toxicol*. 2008;25:442-446.
- Anserini P, Chiodi S, Spinelli S, et al. Semen analysis following allogeneic bone marrow transplantation. Additional data for evidence-based counselling. *Bone Marrow Transplant*. 2002;30:447-451.
- Fang F, Ni K, Cai Y, et al. Busulfan administration produces toxic effects on epididymal morphology and inhibits the expression of ZO-1 and vimentin in the mouse epididymis. *Biosci Rep*. 2017;37:BSR20171059.
- Kidder GM, Cyr DG. Roles of connexins in testis development and spermatogenesis. *Semin Cell Dev Biol*. 2016;50:22-30.
- Gerber J, Heinrich J, Brehm R. Blood-testis barrier and Sertoli cell function: lessons from SCCx43KO mice. *Reproduction*. 2016;151:R15-R27.
- Sridharan S, Simon L, Meling DD, et al. Proliferation of adult sertoli cells following conditional knockout of the Gap junctional protein GJA1 (connexin 43) in mice. *Biol Reprod*. 2007;76:804-812.
- Naiki-Ito A, Asamoto M, Naiki T, et al. Gap junction dysfunction reduces acetaminophen hepatotoxicity with impact on apoptotic signaling and connexin 43 protein induction in rat. *Toxicol Pathol*. 2010;38:280-286.
- Ogawa K, Pitchakarn P, Suzuki S, et al. Silencing of connexin 43 suppresses invasion, migration and lung metastasis of rat hepatocellular carcinoma cells. *Cancer Sci*. 2012;103:860-867.

How to cite this article: Nozaki S, Naiki T, Naiki-Ito A, et al. Selective lysine-specific demethylase 1 inhibitor, NCL1, could cause testicular toxicity via the regulation of apoptosis. *Andrology*. 2020;8:1895-1906. <https://doi.org/10.1111/andr.12846>